Inorganic Chemistry

Article

pubs.acs.org/IC

Mechanistic Studies on the Reaction of Nitroxylcobalamin with Dioxygen: Evidence for Formation of a Peroxynitritocob(III)alamin Intermediate

Harishchandra Subedi[†] and Nicola E. Brasch*[,†,‡]

[†]Department of Chemistry and Biochemistry and [‡]School of Biomedical Sciences, Kent State University, Kent, Ohio 44242, United States

Supporting Information

ABSTRACT: Studies by others suggest that the reduced vitamin B_{12} complex, cob(II)alamin, scavenges nitric oxide to form air-sensitive nitroxylcobalamin (NO^--Cbl(III); NOCbl) in vivo. The fate of newly formed NOCbl is not known. A detailed mechanistic investigation of the oxidation of NOCbl by oxygen is presented. Only base-on NOCbl reacts with O_2, and the reaction proceeds via an associative mechanism involving a peroxynitritocob(III)alamin intermediate, Co(III)-N(O)OO^-. The intermediate undergoes O−O bond homolysis and ligand isomerization to ultimately yield NO_2Cbl and H_2OCbl^+/HOCbl, respectively. Ligand isomerization may potentially occur independent of O−O bond homolysis. Formation of $^{\bullet}OH$ and $^{\bullet}NO_2$ intermediates from O−O bond homolysis is demonstrated using phenol and tyrosine radical traps and the characterization of small amounts of a corrinoid product with minor modifications to the corrin ring.

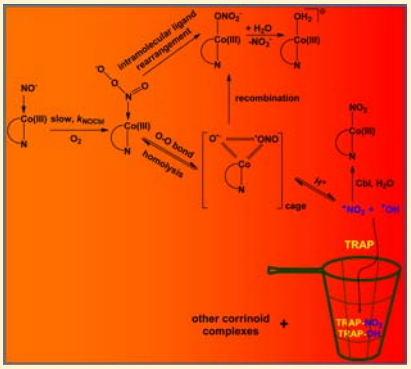

INTRODUCTION

Nitric oxide ($^{\bullet}NO$, NO) is an important cellular signaling molecule produced in cells by nitric oxide synthases (NOS).[1] NO is involved in physiological and pathological processes in mammals, playing a key role in vasodilation, the immune response, neurotransmission, and inhibiting platelet aggregation.[2,3] Vitamin B_{12} derivatives (cobalamins, Cbls) are a class of cobalt-containing macrocyclic complexes synthesized by bacteria which are structurally close to porphyrins, Figure 1. The Co^{3+} NO^- derivative of vitamin B_{12} known as nitrosylcobalamin or nitroxylcobalamin, NO^--Cbl(III),[4] has attracted considerable attention in literature. Both mammalian B_{12}-dependent enzymes, methylcobalamin-dependent methionine synthase, and adenosylcobalamin-dependent L-methylmalonyl-CoA mutase, are inhibited by NO in vitro and in vivo,[5,6] and the inhibition is attributed to the formation of NOCbl.[7] It has been postulated that cobalamins efficiently scavenge NO in vivo to form NOCbl.[7,8] Cob(II)alamin, a major intracellular form of Cbl,[9] reacts with NO at almost diffusion controlled rates to form NOCbl ($k = 7.4 \times 10^8$ M^{-1} s^{-1}, $K_{eq} \approx 1 \times 10^8$ M^{-1}, 25 °C).[10,11] Cbls show potential in treating pathologies associated with elevated NO levels including sepsis/septic shock.[8,12] Cbls also inhibit NO-induced vasodilation[13] and NO-induced smooth muscle relaxation.[14,15] Finally, it has been proposed that NOCbl can act as a chemotherapeutic agent to treat cancer.[16]

NOCbl itself is extremely air sensitive.[10,17,18] Interestingly, others choose not to report this fact when discussing the biological relevance of the trapping of NO by Cbl to form NOCbl, or in studies focused on therapeutic properties of

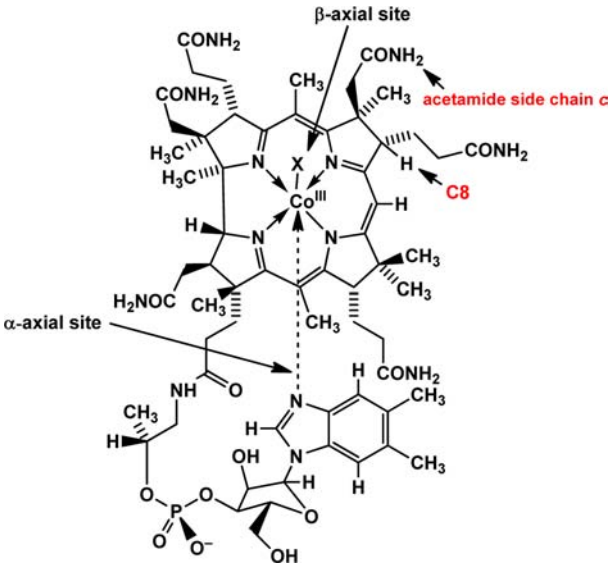

Figure 1. Structure of vitamin B_{12} (cobalamins): X = CN^-, CH_3, Ado, H_2O, NO^-, NO_2^-, etc.

NOCbl.[6,7,13,14,19−21] Furthermore, although UV−vis spectral studies reported by us and others suggest that NOCbl is simply oxidized to nitrocobalamin (NO_2Cbl) by O_2 (although this is not so simple as it initially seems, since it requires cleavage of the O═O bond),[10,17,18,22] studies by others on the reactions of

Received: July 30, 2013
Published: September 19, 2013

other NO^-−Co(III) complexes with O_2 suggest that the mechanism is complex, with multiple products produced under some conditions.[23] Herein, we present a detailed mechanistic study of the reaction between NOCbl and O_2, which provides support for formation of a peroxynitrito Co(III) intermediate.

EXPERIMENTAL SECTION

Materials and Methods. *Chemicals.* Hydroxycobalamin hydrochloride (HOCbl·HCl, 98% stated purity by the manufacturer) was purchased from Fluka. All biological buffers (MES, TES, TAPS, and CAPS) and inorganic buffers (CH_3COONa, NaH_2PO_4, or Na_2HPO_4), D_2O (99.8 atom % D), KCN (99%), acetone, glacial acetic acid (HPLC grade), triflic acid, ammonium hydroxide, NaOH, phenol (≥99%), catechol (99%), 2-nitrophenol (99%), 4-nitrophenol (98%), *L*-tyrosine (≥99%), *n*-octylamine (≥99%), tetrabutylammonium hydrogen sulfate (99%), sodium nitrate (≥99%), sodium dithionite (85%), and HPLC grade water and acetonitrile were purchased from either Fisher Scientific or Acros Organics. Hydroquinone (≥99%), 3,4-dihydroxy-*L*-phenylalanine (≥98%), 3-nitro-*L*-tyrosine (≥98%), TSP (3-(trimethylsilyl)propionic 2,2,3,3-d_4 acid, sodium salt) and methanol (HPLC grade) were obtained from Sigma Aldrich. 2-(*N*,*N*-diethylamino)-diazenolate 2-oxide (DEA-NONOate, Na^+ salt, ≥98%) was purchased from Cayman Chemical. Water was purified using a Barnstead Nanopure Diamond water purification system.

Synthesis of NOCbl. NOCbl was prepared under anaerobic conditions inside the glovebox using a published procedure.[18] The formation of NOCbl product was confirmed by ^{1}H NMR and UV−vis spectroscopy.

Synthesis of NO_2Cbl. NO_2Cbl was prepared following a procedure reported in the literature.[22] ^{1}H NMR and UV−vis spectroscopy were used to characterize NO_2Cbl and check its purity.

General Methods. *Solution Preparations.* All solutions were prepared using standard biological buffers and inorganic buffers (acetate and phosphate; 0.10 M) and a constant ionic strength was maintained using sodium triflate ($NaCF_3SO_3$; I = 1.0 M). Air-saturated solutions were prepared by bubbling air through the solutions for at least ∼6 h. Air-free solutions were prepared by bubbling argon for ∼24 h. Air-sensitive solutions were stored in the MBRAUN Labmaster 130 (1250/78) glovebox filled with argon, equipped with O_2 and H_2O sensors and a freezer at −24 °C. Solutions of varying oxygen concentration were prepared by mixing air-saturated buffer solution ($[O_2] = 1.22 \times 10^{-3}$ M at 25 °C[24]) and deoxygenated buffer solution in different proportions.

Determination of Cbl Concentrations. The percentage of water in HOCbl·HCl (·$n$$H_2O$) was determined by converting HOCbl·HCl to dicyanocobalamin, $(CN)_2Cbl^-$ (0.10 M KCN, pH 11.0, $\varepsilon_{368\ nm} = 3.04 \times 10^4$ M^{-1} cm^{-1}).[25] NOCbl concentrations in stock solutions were determined using the same procedure. Alternatively, concentrations were determined by UV−vis spectrometry (extinction coefficient for NOCbl at 478 nm, $\varepsilon_{478\ nm} = 6.91 \times 10^3$ M^{-1} cm^{-1}).[18]

pH Measurements. All pH measurements were carried out at room temperature using an Orion Model 710A pH meter equipped with a Mettler-Toledo Inlab 423 or 421 electrodes. The electrode was filled with 3 M KCl/saturated AgCl solution (pH 7) and calibrated with standard buffer solutions at pH 4.00, 7.00, 10.00, and 12.45.

Kinetic Experiments. Air-free UV−vis spectrometric measurements were carried out in Schlenk cuvettes (cuvettes fitted with a J-Young or an equivalent stopcock) on a Cary 5000 spectrophotometer equipped with a thermostatted (25.0 ± 0.1 °C) cell changer operating with WinUV Bio software (version 3.00). Freshly prepared solutions were used for kinetic measurements. For rapid reactions, kinetic data were collected under strictly anaerobic conditions at 25.0 ± 0.2 °C using an Applied Photophysics SX20 stopped-flow instrument equipped with a photodiode array detector, operating with Pro-Data SX (version 2.1.4) and Pro-Data Viewer (version 4.1.10) software, with either a 2 or a 10 mm path length cell. The instrument was continuously purged with nitrogen gas during data collection and pretreated with aqueous anaerobic sodium dithionite (5×10^{-3} M) to remove oxygen for at least 1 h prior to thoroughly washing with anaerobic water. Hamilton gastight syringes filled with the anaerobic reactant solutions in the glovebox were used to introduce the reactant solutions into the reservoir syringes of the stopped-flow instrument. Data were fitted using the program Microcal Origin version 8.0.

^{1}H NMR Measurements. ^{1}H NMR spectra were recorded on a Bruker 400 MHz spectrometer equipped with a 5 mm probe at 23 ± 1 °C. TSP was used as internal reference. For ^{1}H NMR experiments under anaerobic conditions, airtight J-Young NMR tubes (Wilmad, 535-JY-7) were used. Reaction mixtures were equilibrated for 15 min prior to measurements.

HPLC Experiments. HPLC analyses were carried out in an Agilent 1100 series HPLC system equipped with a degasser, quaternary pump, autosampler, and a photodiode array detector (resolution of 2 nm).

Method A. A Phenomenex Luna C_{18} semipreparative column (5 μm, 100 Å, 10 mm × 250 mm) was used. Peaks were monitored at 254, 280, and 350 nm and a mobile phase consisting of acetic acid buffer (0.1% v/v in H_2O, pH adjusted to 4.0 with 4.0 N NH_4OH), **A**, and 0.1% acetic acid (v/v) in pure CH_3CN (pH not adjusted), **B** was used. *Gradient conditions:* 0−2 min, 95:5 **A:B** (isocratic); 2−14 min, linear gradient to 85:15 **A:B**; 14−19 min, linear gradient to 82:18 **A:B**; 19−32 min, linear gradient to 65:35 **A:B**; 32−33 min, linear gradient to 40:60 **A:B**; 33−35 min, linear gradient to 95:5 **A:B**; 35−37 min, 95:5 **A:B** (isocratic). A flow rate of 3 mL/min was used in all experiments.

Method B. For tyrosine radical trap experiments, an Alltech Alltima (Grace) C_{18} semipreparative column (5 μm, 100 Å, 10 mm × 300 mm) was used. Peaks were monitored at 220, 254, 280, and 350 nm and a mobile phase consisting of acetic acid buffer (0.1% v/v in H_2O, pH adjusted to 4.0 ± 0.1 with 4.0 N NH_4OH), **A**, and pure CH_3OH, **B** was used. *Gradient conditions:* 0−2 min, 70:30 **A:B** (isocratic); 2−5 min, linear gradient to 60:40 **A:B**; 5−27 min, linear gradient to 55:45 **A:B**; 27−30 min, linear gradient to 70:30 **A:B** and 30−32 min, 70:30 **A:B** (isocratic). A flow rate of 3 mL/min was used in all experiments. All the solutions for tyrosine derivatives were prepared in 0.1 M phosphate buffer; pH 7.40 and diluted as needed. The tyrosine solution was sonicated for 15 min to increase its solubility in aqueous solution.

Method C. For phenol radical trap experiments, a Phenomenex Luna C_{18} analytical column (5 μm, 100 Å, 4.6 mm × 250 mm) was used. Peaks were monitored at 254, 280, 315, and 350 nm and a mobile phase consisting of acetic acid buffer (0.1% v/v in H_2O, pH adjusted to 4.0 with 4.0 N NH_4OH), **A**, and 0.1% acetic acid (v/v) in pure CH_3CN (pH not adjusted), **B** was used. *Gradient conditions:* 0−2 min, 95:5 **A:B** (isocratic); 2−14 min, linear gradient to 85:15 **A:B**; 14−19 min, linear gradient to 82:18 **A:B**; 19−45 min, linear gradient to 45:55 **A:B**; 45−50 min, linear gradient to 20:80 **A:B**; 50−52 min, linear gradient to 95:5 **A:B**; 52−53 min, 95:5 **A:B** (isocratic). A flow rate of 1 mL/min was used in all experiments. All the solutions for phenol standards (phenol, catechol, hydroquinone, 2-nitrophenol and 4-nitrophenol) were prepared in 0.1 M phosphate buffer; pH 7.40 and diluted as needed.

Method D. An isocratic method (94:6 **A:B**; 3 mL/min flow rate) was used. The solvents and HPLC column used were the same as in Method A.

Method E. For NO_3^- detection experiments, an HPLC method reported in the literature was used with minor modifications.[26,27] A Phenomenex Luna C_{18} analytical column (5 μm, 100 Å, 4.6 mm × 250 mm) was used. Peaks were monitored at 220, 280, and 350 nm, and a mobile phase consisting of 0.01 M *n*-octylamine (pH adjusted to 6.6 with 4.0 M CH_3COOH), **A**, and pure CH_3OH, **B** was used. An isocratic method (80:20 **A:B**; 1 mL/min flow rate) was used.

For HPLC experiments, the product mixture of the reaction between NOCbl with O_2 was prepared as follows: solid NOCbl was dissolved in anaerobic phosphate buffer (0.10 M, pH 7.40) inside the glovebox and removed from the glovebox to expose the sample to air. Tyrosine and phenol were added as needed prior to exposing the sample to air.

HPLC chromatograms of authentic samples of cobalamins (H_2OCbl^+ and NO_2Cbl), phenols (phenol, catechol, hydroquinone, 2-nitrophenol and 4-nitrophenol), tyrosines (tyrosine (Tyr), 3-

dx.doi.org/10.1021/ic401975f | Inorg. Chem. 2013, 52, 11608−11617

hydroxytyrosine (OH-Tyr) and 3-nitrotyrosine (NO_2-Tyr)), and nitrate ($NaNO_3$) were independently run to determine the exact retention times for these species. Chromatograms for these standards are given in the Supporting Information. Duplicate HPLC experiments were carried out, giving identical results.

Mass Spectrometry Identification of Unknown HPLC Peak in the Product Mixture of the Reaction of NOCbl with O_2. HPLC fractions were collected, combined, and the pH of the solution (~ 40 mL) was adjusted to 7.10. The solution was taken to dryness using rotary evaporator. The pH of the solution was readjusted to 7.2 (from 6.0) when the volume of the solution was ~4 mL during the evaporation process (cobalamins are prone to corrin ring destruction and amide hydrolysis under highly acidic conditions[28]). ESI-MS (+ve mode) measurements were carried out using an Agilent 6220 Time of Flight (TOF) instrument equipped with a multimode source (MMI) at the Central Instrumentation Facilities in the Department of Chemistry at Colorado State University.

Determination of the Equilibrium Constant for the Reaction of NOCbl with O_2. Varying amounts of an air-saturated buffered solution (0.10 M phosphate buffer; pH 7.40) were injected using a gastight syringe into an anaerobic solution of NOCbl in phosphate buffer (0.10 M, pH 7.40, final conc. 1.00×10^{-4} M) in HPLC vials (~1.8 mL) capped with a septum screw cap. The final volume of the solution was 1.5 mL. The reaction was allowed to proceed to completion for 2 h, and each product solution subsequently diluted to 4.50×10^{-5} M Cbl with anaerobic phosphate buffer solution (0.10 M phosphate buffer; pH 7.40) inside the glovebox before recording the UV–vis spectrum. Selected spectra were repeated, and the data found to be reproducible to within ±1% absorbance units.

Probing for Possible Cbl Reaction Intermediates by ^{1}H NMR Spectroscopy. An aliquot of air-saturated buffer (0.50 equiv of O_2, 0.10 M phosphate buffer, pD 7.40) was injected into an anaerobic NOCbl solution (final conc. 1.00×10^{-3} M, 0.10 M phosphate buffer, pD 7.40), and the product mixture was transferred to an air-free NMR tube after 15 min to record the ^{1}H NMR spectrum.

RESULTS

Kinetic Studies. Upon addition of air-saturated buffer (O_2 = 1.22×10^{-3} M at 25 °C[24]) to a solution of NOCbl, UV–vis spectral scans show that NOCbl (λ = 318 and 478 nm[10]) is cleanly converted to species with spectral features characteristic of nitrocobalamin (λ = 352, 410, and 526 nm[22]), Figure 2 (pH 7.40, 0.10 M TES buffer, I = 1.0 M; $NaCF_3SO_3$). However the UV–vis spectra of aquacobalamin/hydroxycobalamin (H_2OCbl^+/HOCbl, pK_a(H_2OCbl^+) = 7.8;[22] λ_{max} = 351, 412, and 526 nm at pH 7.4) and NO_2Cbl (λ = 354, 413, and 531 nm at pH 7.4) are practically indistinguishable.[22] ^{1}H NMR spectroscopy is a useful tool to distinguish between these complexes, since Cbls have 5 characteristic chemical shifts in the aromatic region which are strongly dependent on the β-axial ligand.[22,29] The ^{1}H NMR spectrum of a NOCbl solution (1.00×10^{-3} M, 0.10 M phosphate buffer, pD 7.40) solution exposed to air show that *both NO_2Cbl and H_2OCbl^+/HOCbl are formed*, in a ~ 37:63 ratio (±2%; mean value of 3 experiments), Figure 3.

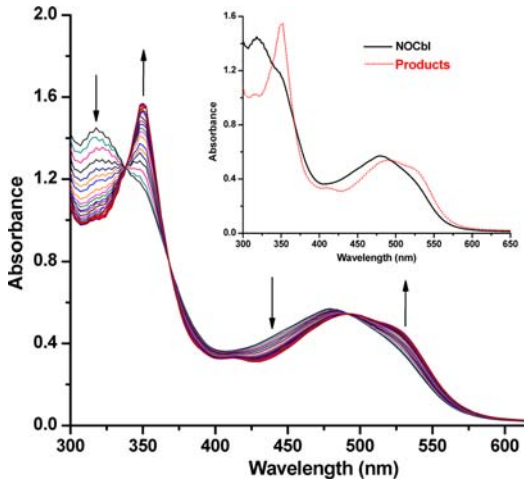

Figure 2. UV–vis spectra for the reaction between NOCbl (5.00×10^{-5} M) and excess O_2 (6.10×10^{-4} M) at pH 7.40 ± 0.02 (25.0 °C, 0.10 M TES buffer, I = 1.0 M; $NaCF_3SO_3$). Spectra were recorded every 0.25 s. **Inset:** Initial spectrum (= NOCbl) and final spectrum (= products).

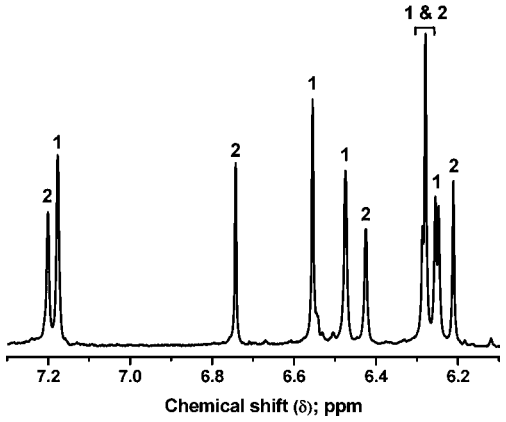

Figure 3. ^{1}H NMR spectrum of a solution of NOCbl (1.00×10^{-3} M) exposed to air for 30 min (pD 7.40, 0.10 M phosphate buffer). The peaks at 7.17, 6.55, 6.47, 6.28, and 6.24 ppm correspond to H_2OCbl^+/HOCbl (**1**) and those at 7.19, 6.74, 6.42, 6.27, and 6.21 ppm correspond to NO_2Cbl (**2**). From the integration of the peaks, the ratio of (H_2OCbl^+/HOCbl):NO_2Cbl is ~63:37.

The HPLC chromatogram of this same NMR solution and an aqueous solution of NOCbl (1.00×10^{-4} M, 0.10 M phosphate buffer, pH 7.40) exposed to air also show formation of NO_2Cbl/(H_2OCbl^+/HOCbl), Figure 4. The fraction of NO_2Cbl observed by HPLC is smaller than that observed by ^{1}H NMR spectroscopy, because of partial decomposition of NO_2Cbl on the HPLC column. This was confirmed by injecting an authentic sample of NO_2Cbl, Supporting Information, Figure S1. Hence both ^{1}H NMR spectroscopy and HPLC clearly show that NOCbl is oxidized by air to form a NO_2Cbl/(H_2OCbl^+/HOCbl) mixture, rather than simple conversion to NO_2Cbl. In Figure 4 an additional small corrinoid peak is observed in the HPLC chromatogram at 350 nm immediately prior to elution of H_2OCbl^+, whose identity will be discussed in detail later.

Kinetic measurements were carried out on the reaction between NOCbl and O_2 under pseudo-first-order conditions. Figure 5 gives a plot of absorbance at 315 nm versus time for the reaction of NOCbl (7.50×10^{-5} M) with O_2 (1.00×10^{-5} M) at pH 7.40 (25.0 °C, 0.10 M TES buffer, I = 1.0 M; $NaCF_3SO_3$). The data fit well to a single first-order rate equation giving an observed rate constant, k_{obs} = (3.89 ± 0.01) $\times 10^{-2}$ s^{-1}. Data were collected at other NOCbl concentrations, with at least 7.5 times excess NOCbl compared to the concentration of oxygen, to achieve essentially pseudo-first-order conditions. Keeping NOCbl rather than O_2 in excess improved the reproducibility of the rate constants. A second-order rate constant (k_{app}) was calculated from the plot of k_{obs}

dx.doi.org/10.1021/ic401975f | Inorg. Chem. 2013, 52, 11608–11617

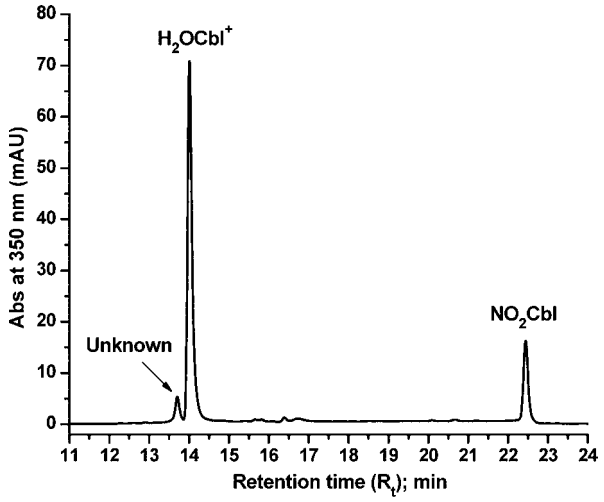

Figure 4. HPLC chromatogram for the products of the reaction between NOCbl (1.00×10^{-4} M) and O_2 (air) at pH 7.40 (0.10 M, phosphate buffer, 25.0 °C). The peaks at 14.0 and 22.4 min correspond to H_2OCbl^+ (~74%) and NO_2Cbl (~26%), respectively. H_2OCbl^+ and NO_2Cbl amounts are estimated using peak areas and molar extinction coefficients at 350 nm. An unknown corrinoid complex elutes at 13.7 min.

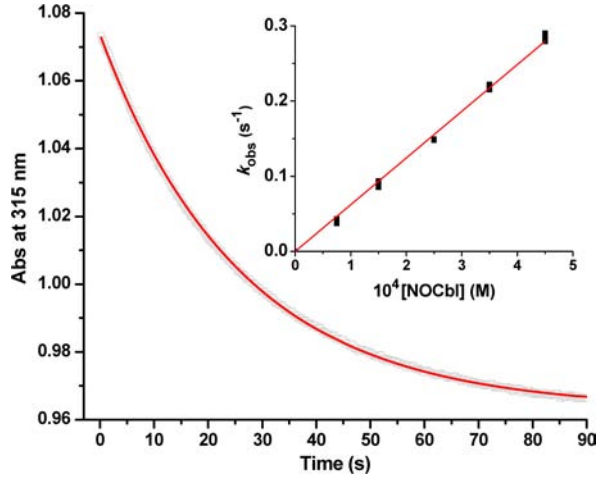

Figure 5. Plot of absorbance at 315 nm versus time for the reaction of NOCbl (7.50×10^{-5} M) with O_2 (1.00×10^{-5} M) at pH 7.40 ± 0.02 (25.0 °C, 0.10 M TES buffer, I = 1.0 M; $NaCF_3SO_3$). The first order fit of the data gives the observed rate constant (k_{obs}) = (3.89 ± 0.01) × 10^{-2} s^{-1}. **Inset:** Plot of k_{obs} versus [NOCbl] for the same reaction giving a second-order rate constant (k_{app}) = 621 ± 6 M^{-1} s^{-1}.

versus NOCbl concentration (inset to Figure 5). A straight line passing through the origin is consistent with the rate-determining step involving the reaction of O_2 with NOCbl, giving an apparent second-order rate constant, k_{app} = 621 ± 6 M^{-1} s^{-1} at pH 7.40.

Similar experiments were carried out at other pH conditions and k_{app} values determined from plots of k_{obs} versus [NOCbl] at each pH condition, Supporting Information, Figures S2–S8. Figure 6 summarizes the results. The reaction rate increases with increasing pH to become pH independent for pH > 7. Importantly, in acidic aqueous solution NOCbl exists in a mixture of its "base-on" (the *N*-bound 5,6-dimethylbenzimidazole (DMB) is coordinated at the α-axial site of the Cbl) and "base-off" form (a water displaces the 5,6-dimethylbenzimidazole from the α-axial site), Scheme 1. The data in Figure 6 were fitted to eq 1 assuming that only base-on NOCbl, not the two

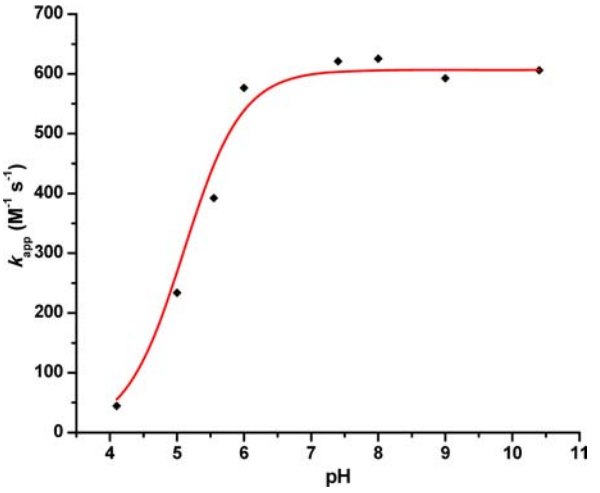

Figure 6. Plot of second-order rate constant (k_{app}) versus pH for the reaction between NOCbl and O_2. The data have been fitted to eq 1 in the text fixing $pK_{base\text{-}off}$(NOCbl) = 5.1 and K_{Co} = 1.9, giving the rate constant (k_{NOCbl}) = 926 ± 20 M^{-1} s^{-1}.

Scheme 1. Base-on and Base-off Forms of NOCbl Formed in Aqueous Solution

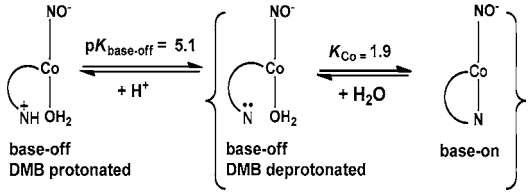

base-off complexes, reacts with O_2, with the value of $pK_{base\text{-}off}$(NOCbl) fixed to 5.1[10] and K_{Co} fixed to 1.9.[4] The best fit of the data in Figure 6 to eq 1 gives the rate constant, k_{NOCbl} = 926 ± 20 M^{-1} s^{-1}. The role of the ligand *trans* to the NO^- with respect to the reactivity of nitroxyl cobalt complexes with O_2 is well established, with strong σ donating ligands significantly increasing the rate of the reaction.[23,30]

$$k_{NOCbl} = \frac{k_{app}K_{base\text{-}off}K_{Co}}{(10^{-pH} + K_{base\text{-}off})(K_{Co} + 1)} \quad (1)$$

To determine the thermodynamic parameters $\Delta H^{\ddagger}$ and $\Delta S^{\ddagger}$, temperature dependence studies were carried out for the reaction of NOCbl with O_2 in the 15.0–45.0 °C range at pH 7.40 ± 0.02. Under these conditions NOCbl exists in its base-on form. Figure 7 gives the Eyring plot of ln (k/T) versus $1/T$. The slope and intercept of the plot give $\Delta H^{\ddagger}$ = 29 ± 1.4 kJ mol^{-1} and $\Delta S^{\ddagger}$ = −94.0 ± 4.2 J K^{-1} mol^{-1}, respectively.

Determination of the Equilibrium Constant (K_{eq}). Equilibrated solutions of NOCbl (1.00×10^{-4} M) with varying numbers of equivalents of O_2 (0–12.2 equiv) were prepared, and the product solutions diluted to 4.50×10^{-5} M before recording UV–vis spectra, Figure 8. Note that scatter in the absorbance spectra is observed, since individual solutions were prepared for each O_2 concentration and transferred one by one to a cuvette to record the UV–vis spectrum. From a plot of absorbance at 352 nm versus concentration of O_2 (inset to Figure 8), it is clear that the reaction requires excess O_2 to

dx.doi.org/10.1021/ic401975f | Inorg. Chem. 2013, 52, 11608–11617

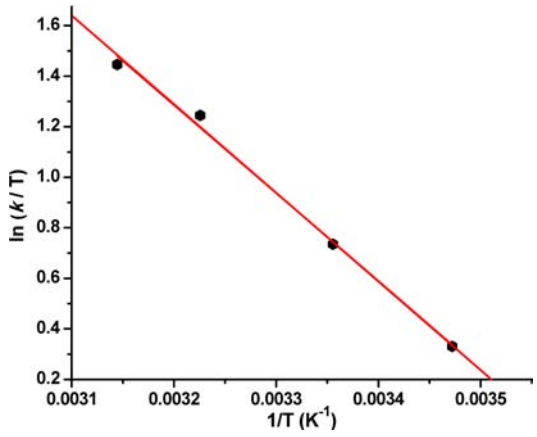

Figure 7. Plot of ln (k/T) versus $1/T$ (Eyring plot) for the reaction of NOCbl with O_2 at pH 7.40 ± 0.02 (0.10 M TES buffer, I = 1.0 M; $NaCF_3SO_3$). The slope and the intercept of the Eyring plot give $\Delta H^{\ddagger}$ = 29 ± 1.4 kJ mol^{-1} and $\Delta S^{\ddagger}$ = −94.0 ± 4.2 J K^{-1} mol^{-1}, respectively.

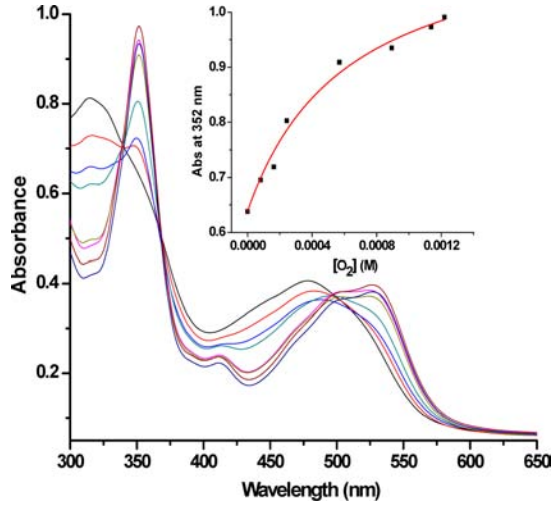

Figure 8. UV−vis spectra for equilibrated solutions of NOCbl (1.00×10^{-4} M) with varying numbers of equivalents of O_2 (0−12.2 equiv) at pH 7.40 (0.10 M phosphate buffer) at 25.0 °C. **Inset:** Plot of absorbance at 352 nm versus $[O_2]$. The best fit of the data to eq 2 in the text gave an equilibrium constant, K_{eq} = (1.62 ± 0.34) × 10^3 M^{-1}.

proceed to completion. The data were fitted to eq 2. A_0 and A_∞ represent the absorbance in the absence of O_2 and the absorbance after the complete formation of products, respectively, and A_{obs} is the observed absorbance at a specific O_2 concentration. The best fit of the data to eq 2 gave an equilibrium constant (K_{eq}) of (1.62 ± 0.34) × 10^3 M^{-1} (pH 7.40).

$$A_{obs} = (A_0 + A_\infty K_{eq}[O_2])/(1 + K_{eq}[O_2]) \quad (2)$$

Probing for Reaction Intermediates. 0.50 mol equiv of O_2 was added to an anaerobic solution of NOCbl (1.00×10^{-3} M), and the ^{1}H NMR spectrum of the product mixture recorded (pD 7.40). Three sets of Cbl peaks were observed in the product mixture corresponding to unreacted NOCbl and the NO_2Cbl and H_2OCbl^+/HOCbl products, Supporting Information, Figure S9. Hence significant amounts of other Cbl complexes are not observed by ^{1}H NMR spectroscopy with the addition of less than 1 mol equiv of O_2.

It has been proposed that a transition metal-bound peroxynitrite intermediate is formed upon reacting nitrosyl transition metal complexes with O_2 (see below).[23,30−35] This complex may decompose to generate NO_3^-, $^{\bullet}$OH, and $^{\bullet}NO_2$ intermediates.[31,32,36,37] HPLC experiments showed that NO_3^- is present in the product mixture, Supporting Information, Figure S10, in an amount consistent with the (H_2OCbl^+/HOCbl):NO_2Cbl product ratio of ∼63:37. Experiments were also carried out to probe for formation of other noncobalamin corrinoid products, which may arise as a result of $^{\bullet}$OH and/or $^{\bullet}NO_2$ intermediates attacking the corrin ring of the Cbl complex. The product mixture of the reaction between NOCbl (1.00×10^{-3} M) and O_2 was treated with excess solid KCN (pH > 10) to convert all corrinoid complexes to their dicyano forms. The pH was subsequently lowered to 3 before bubbling the solution with air to convert dicyanocobalamin ($(CN)_2Cbl^-$) to CNCbl and to remove excess cyanide (as HCN).[25] Figure S11 in the Supporting Information shows a major peak (∼ 96% at 280 nm) in the HPLC chromatogram of the product mixture, with a retention time and UV−vis spectrum identical to CNCbl. This suggests that almost all of the corrinoid products are cobalamin complexes. HPLC fractions for this peak were collected and taken to dryness. ESI-MS confirmed that this peak does indeed correspond to CNCbl; that is, corrin ring modifications are not present to any significant extent in the major cobalamin products ((H_2OCbl^+/HOCbl) + NO_2Cbl), Supporting Information, Figure S12.

To further investigate whether the free radicals $^{\bullet}$OH and $^{\bullet}NO_2$ are formed in solution upon reacting NOCbl with O_2, the products of the reaction between NOCbl and O_2 were determined in the presence of the established $^{\bullet}$OH/$^{\bullet}NO_2$ trapping agent phenol. Phenol traps the $^{\bullet}$OH and $^{\bullet}NO_2$ intermediates formed upon the spontaneous decomposition of ONOOH in aqueous solution (pH 6.8) to form hydroquinone (3%), catechol (0.2%), 2-nitrophenol (3%), and 4-nitrophenol (2.2%).[38,39] An HPLC method was developed suitable for separating the hydroxylated and nitrated phenol derivatives from phenol, Supporting Information, Figure S13. A control experiment showed that formation of 1% (relative to the Cbl concentration) hydroquinone, catechol, 4-nitrophenol, and 2-nitrophenol would be detectable in the HPLC chromatogram of the product mixture, Supporting Information, Figure S14. Both 4-nitrophenol (33.3 min, < 1%; no attempt was made to quantitate the amounts of the phenol products) and 2-nitrophenol (38.7 min, < 1%) were clearly observed in the HPLC chromatogram of the products of the reaction of NOCbl with air in the presence of excess phenol (0.10 M), Figure 9, indicating that free $^{\bullet}NO_2$ radicals are formed during the reaction. However, hydroxylated phenol derivatives (hydroquinone and catechol) proved more difficult to observe in the presence of the Cbl products. The peak for catechol (17.3 min) overlaps with cobalamin impurities, and hydroquinone was also not detected.

To probe further for formation of a $^{\bullet}$OH intermediate, a second $^{\bullet}$OH/$^{\bullet}NO_2$ trapping agent, tyrosine (Tyr), was used. Tyr traps the $^{\bullet}$OH and $^{\bullet}NO_2$ intermediates formed during ONOOH decomposition (pH 7.40) to give a much larger yield of the hydroxylated trapped product 3-hydroxytyrosine (OH-Tyr, 9%) in addition to 3-nitrotyrosine (NO_2-Tyr, 5%).[40−45] Control experiments showed that both OH-Tyr (3%) and (NO_2-Tyr) (3%) are detected in the presence of the Cbl reaction products, Supporting Information, Figure S15. When NOCbl (1.00×10^{-3} M) was reacted with air in the presence of

dx.doi.org/10.1021/ic401975f | Inorg. Chem. 2013, 52, 11608−11617

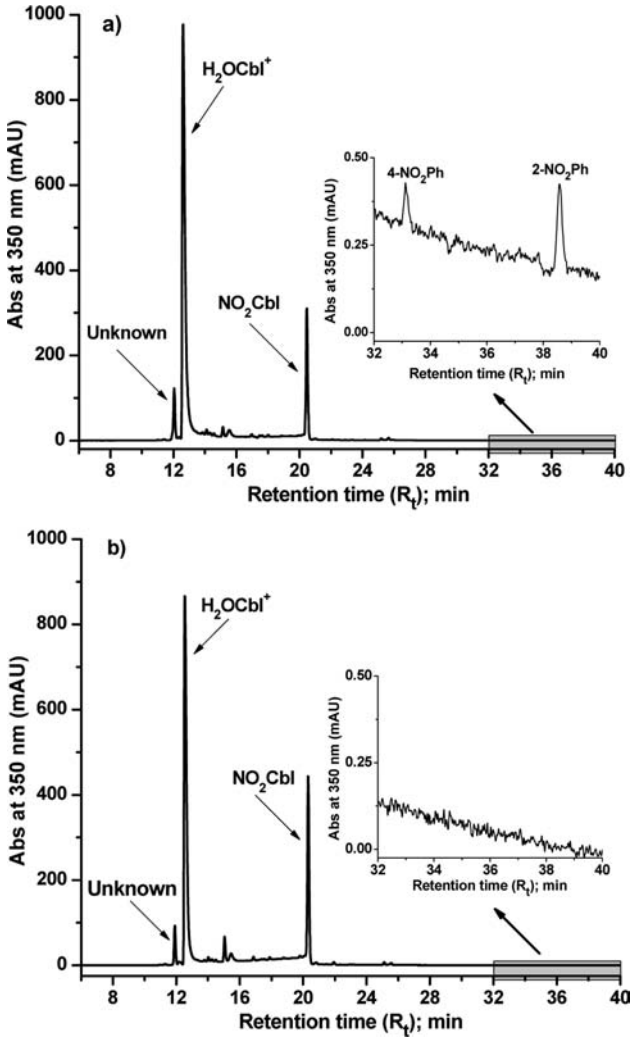

Figure 9. HPLC chromatogram for the products of the reaction between NOCbl (1.00×10^{-3} M) and O_2 (air) in the (a) presence and (b) absence of excess phenol (0.10 M). The prominent peaks at 12.0, 12.6, and 20.5 correspond to a novel corrinoid complex, H_2OCbl^+ and NO_2Cbl, respectively. Note that the peak for phenol (26.6 min; Supporting Information, Figure S10e) is not observed in Figure 9a since phenol does not absorb at 350 nm. The insets to panels a and b are enlarged representations of the 32−40 min region, showing the presence of 4-nitrophenol (4-NO_2Ph; 33.3 min) and 2-nitrophenol (2-NO_2Ph; 38.7 min) in (a) only. Two further minor corrinoid peaks are observed at 15.0 and 15.5 min, which decrease in relative intensity in the presence of phenol. No attempts were made to characterize these complexes.

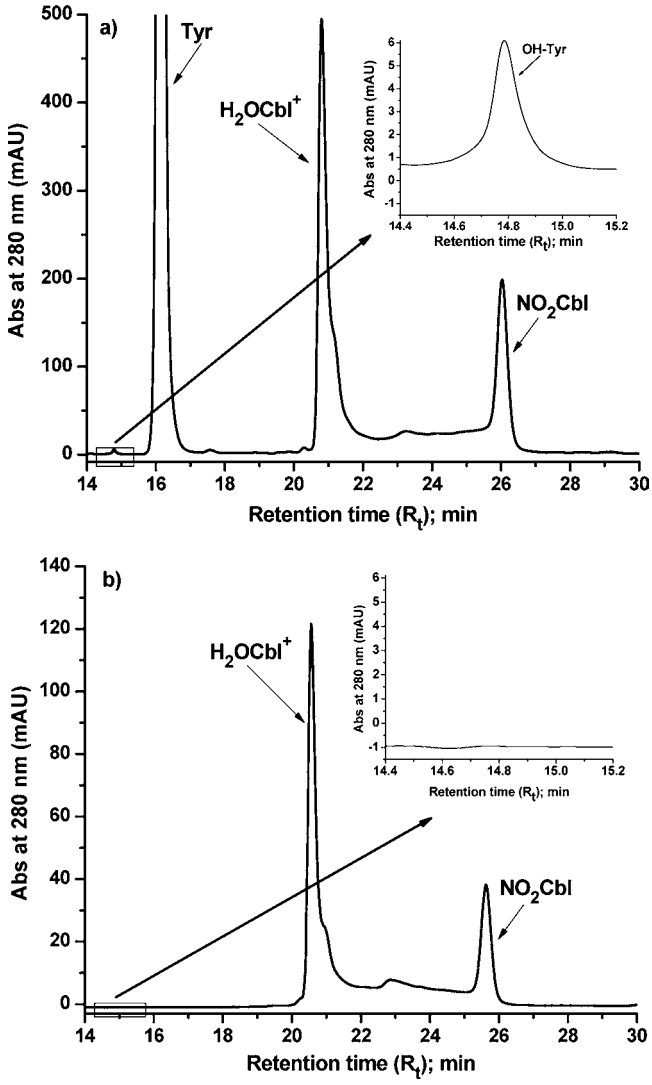

Figure 10. HPLC chromatogram for the products of the reaction of NOCbl (1.00×10^{-3} M) with air in the (a) presence and (b) absence of excess Tyr (6.00×10^{-3} M). The peaks at 14.8, 16.1, 20.8, and 26.0 min correspond to OH-Tyr, Tyr, H_2OCbl^+, and NO_2Cbl, respectively. The insets to panels a and b are enlarged representations of the region where OH-Tyr elutes from the column.

excess Tyr (6.00×10^{-3} M), a small amount (14.8 min, < 1%) of OH-Tyr was clearly observed in the HPLC chromatogram, Figure 10. Using this HPLC method NO_2-Tyr was not observed, most likely because of overlap with Cbl impurities.

An additional small corrinoid peak eluting immediately prior to elution of H_2OCbl^+ was observed at 350 nm in the HPLC chromatogram of the product mixture of the reaction between NOCbl and O_2, Figures 4 and 9, with a UV−vis spectrum indistinguishable from H_2OCbl^+. HPLC fractions of the unknown complex were collected using an isocratic HPLC method to achieve complete separation from H_2OCbl^+, pooled together, and analyzed by mass spectrometry (see Experimental Section and Figures S13f and S16 in the Supporting Information for details). The complex has m/z peaks assignable to a Cbl complex minus two hydrogen atoms, Cbl-2H (observed m/z = 1327.53, calculated m/z for $[(\text{Cbl} -2\text{H}) + \text{H}]^+$, $C_{62}H_{87}CoN_{13}O_{14}P$ = 1327.56) and observed m/z = 664.27 (calculated m/z for $[(\text{Cbl} -2\text{H}) + 2\text{H}]^{2+}$, $C_{62}H_{88}CoN_{13}O_{14}P$ = 664.28)). Although corrinoid ring modifications have been proposed to occur in numerous studies,[28,46,47] typically these complexes are not fully characterized. One possibility is that abstraction of a H atom by a $^{\bullet}OH$ radical at the C8 position (Figure 1) of the corrin occurs. (Unpublished data from our lab shows that $^{\bullet}NO_2$ does not react with the corrin ring.) This results in intramolecular transfer of an unpaired electron to the Co center, and subsequent attack of a deprotonated *N*-amide group of side-chain *c* at the C8 carbocation results in formation of the well-known Co(II) *c*-lactam derivative of aquacobalamin.[28] This complex is oxidized to the corresponding Co(III) complex in the presence of air (a "dehydrovitamin B_{12}" derivative).[48] *c*-Lactam derivatives of B_{12} have very similar UV−vis spectra and chromatographic behavior to the parent B_{12} complexes.[47] Furthermore the *c*-lactam of CNCbl elutes

dx.doi.org/10.1021/ic401975f | *Inorg. Chem.* 2013, 52, 11608−11617

immediately prior to CNCbl on a C18 reverse phase HPLC column, consistent with the retention time of our unknown corrinoid species.[49] However an X-ray structure of the corrinoid product is clearly required to unequivocally characterize this complex, which is beyond the scope of this study.

To summarize, HPLC evidence for formation of $^{\bullet}OH$ and $^{\bullet}NO_2$ radical intermediates was obtained using tyrosine and phenol, respectively, as trapping agents. Observation of a small amount of a (non-Cbl) corrinoid species by HPLC with a retention time close to that of H_2OCbl^+ is also consistent with formation of a $^{\bullet}OH$ intermediate. The amounts of the hydroxylated and nitrated products in the phenol and Tyr trapping experiments were considerably smaller than that observed for ONOO(H) decomposition in the presence of the identical trapping agents. The possibility that $^{\bullet}OH$ and/or $^{\bullet}NO_2$ were instead trapped by the buffer was disproved since the yields of the trapped products were unchanged in the absence of phosphate buffer. Finally, the presence of NO_3^- in the product mixture was also demonstrated using HPLC.

DISCUSSION

Others have proposed formation of a peroxynitrito intermediate upon the oxidation of nitrosyl/nitroxyl metal complexes by oxygen,[23,30−35] eq 3, or the reaction of NO with superoxometal complexes, eq 4.[37,38,50−52]

$$M^{(n-1)+}\text{–NO}/M^{n+}\text{–NO}^- + O_2 \rightarrow M^{n+} - \text{N(O)OO}^- \text{ (or } M^{n+}\text{–OONO}^-) \rightarrow \text{products....} \quad (3)$$

$$M^{(n-1)+}\text{–}O_2/M^{n+}\text{–}O_2^- + NO \rightarrow M^{n+}\text{–OONO}^- \rightarrow \text{products....} \quad (4)$$

Thus far two peroxynitrito complexes have been isolated. Koppenol et al. synthesized $[Co(CN)_5OONO]^{3-}$ by reacting $[Co(CN)_5O_2]^{3-}$ with 1 equiv of $NO_{(g)}$.[38] This complex was remarkably stable in aqueous solution, eventually hydrolyzing. Recently a Cu(I) peroxynitrito complex was synthesized by reacting Cu(II)-NO with H_2O_2.[53] X-ray structures were not reported for either complex.

While peroxynitrite ($ONOO^-$) is relatively stable in solution,[50] ONOOH rapidly undergoes O−O bond homolysis to produce caged $^{\bullet}ONO$ and $^{\bullet}OH$, which recombine to form NO_3^- + H^+, Scheme 2.[54−56] It has also been proposed that direct intramolecular rearrangement of ONOOH occurs, to also yield NO_3^- + H^+.[56] Controversy currently exists concerning the extent of intramolecular rearrangement versus O−O bond homolysis.[54−56] $ONOO^-$ decomposes much more slowly via similar reaction pathways, Scheme 2.

Given that pK_a(ONOOH) is 6.8[57] and that the pK_a of a ligand lowers upon coordination of the ligand to a metal center,[58] it is likely that the intermediate is Co(III)-N(O)OO^- rather than Co(III)-N(O)OOH in the pH range of our study. From kinetic studies on the reaction of NOCbl with O_2 it was found that the rate-determining step is first-order in both [NOCbl] and [O_2], and that only base-on NOCbl, not base-off NOCbl, reacts with O_2 (k_{NOCbl} = 926 ± 20 M^{-1} s^{-1}, 25.0 °C, pH 7.40, 0.10 M phosphate buffer, I = 1.0 M; $NaCF_3SO_3$). Others have also observed that the presence of strong base coordinated *trans* to the nitrosyl group of cobalt nitrosyl

Scheme 2. Decomposition Pathways for ONOOH and $ONOO^-$[a]

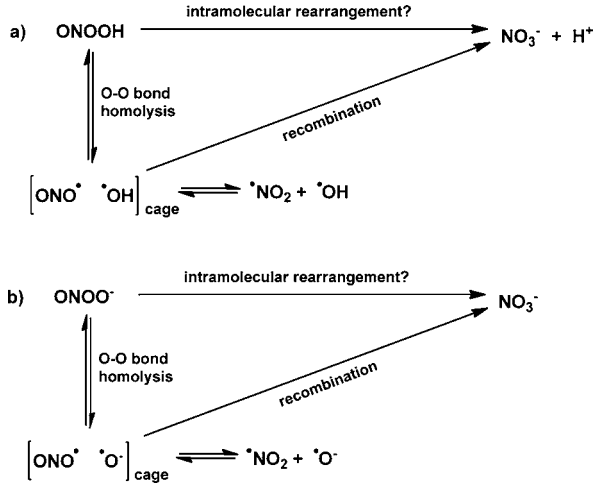

[a]ONOOH also reacts with $ONOO^-$ to produce $2NO_2^-$ + O_2.[56]

complexes leads to an accelerated rate of reaction with O_2,[23,30,59] and the same is also true for other metal-NO complexes.[60] Reaction intermediates were not observed for the NOCbl + O_2 reaction even with 0.5 equiv of O_2, consistent with rate-determining electrophilic attack of O_2 on NOCbl, with subsequent rapid reactions to generate the H_2OCbl^+/HOCbl and NO_2Cbl products. An overall equilibrium constant of (1.62 ± 0.34) × 10^3 M^{-1} was determined at pH 7.40 (25.0 °C). Interestingly, others have reported that the reaction between Co-NO and $^1/_2O_2$ was stoichiometric,[30] and several additional experiments were carried out by us to confirm that this is not the case for the NOCbl + O_2 reaction. On retrospect this result is expected, given that in solution the base-off, 5,6-dimethylbenzimidazole (DMB) deprotonated form of NOCbl exists in equilibrium with base-on NOCbl, Scheme 1,[4] and since H_2O is a weak *trans* σ donor ligand, the base-off complex is unlikely to react with O_2.

Others have proposed for their systems that the nitrosyl ligand initially dissociates from the metal center followed by formation of the superoxometal complex which subsequently reacts with NO to form an *O*-bound peroxynitritometal complex.[31,32,34,35] It has also been suggested that oxygen is first reduced by the metal center of a Re-NO complex to superoxide, which then reacts with the metal complex to form an *N*-bound peroxynitritorhenium intermediate.[33] However these reaction pathways seem unlikely for the NOCbl/O_2 system since the rate-determining step is first-order in both the NOCbl and O_2 concentrations. Furthermore a large negative value of $\Delta S^{\ddagger}$ supports an associative rate-determining step for the reaction between NOCbl and O_2, consistent with electrophilic attack of O_2 on the N of NOCbl to form a *N*-bound peroxynitrito complex. A bimolecular mechanism for formation of the corresponding nitro-Co(III) complex from the peroxynitritocobalt(III) intermediate has been proposed by others, with Co(III)-bound peroxynitrite reacting with Co(III)-NO^- to give NO_2Cbl, Scheme 3.[30,31] If the reaction proceeds via this type of reaction pathway, the NO_2Cbl:(H_2OCbl^+ + HOCbl) product ratio will be dependent on the total cobalamin concentration,[31] with more NO_2Cbl expected at higher cobalamin concentrations. However, HPLC experiments showed that the NO_2Cbl:H_2OCbl^+ product ratio is the same

dx.doi.org/10.1021/ic401975f | Inorg. Chem. 2013, 52, 11608−11617

Scheme 3. Proposed Mechanism for Formation of Nitrocobalamin (NO_2Cbl) Product from the Peroxynitritocobalt(III) Intermediate

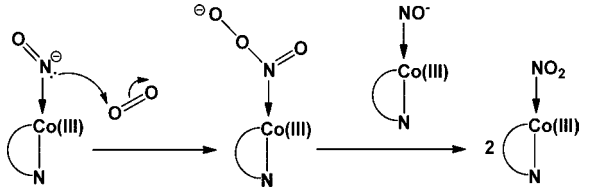

within experimental error for products of the reaction between NOCbl and air at 1×10^{-4} or 1×10^{-3} M Cbl concentrations, which does not support the involvement of a second Co(III) complex in NO_2Cbl formation. Note that this type of mechanism was initially proposed prior to more recent studies showing that ONOOH decomposes via O−O bond homolysis to give $^{\bullet}NO_2$ and $^{\bullet}OH$.[30]

NO_3^- does not bind appreciably to the Co(III) center of cobalamins;[28] therefore any NO_3Cbl potentially formed from isomerization of Co-$ONOO^-$ will decompose to H_2OCbl^+/HOCbl and NO_3^-. Note that formation of the corresponding nitrato complex has been observed for the reaction of the nitrosyl cobaloxime complex $BCo(DH)_2NO$ (B = base) with O_2 and for the reaction of other metal nitrosyl complexes with O_2.[23] The observation of ∼37% NO_2Cbl suggests that like ONOOH and $ONOO^-$, Co(III)-bound $ONOO^-$ decomposes by O−O homolysis. Ligand isomerization ultimately gives H_2OCbl^+/HOCbl after dissociation of the ONO_2^- ligand, although it is not clear to us if this occurs via direct intramolecular rearrangement of the ligand in addition to O−O bond homolysis and recombination of the caged radical species. Others have reported that light can affect the products observed for the hydrolysis of a Co(III)-$OONO^-$ complex, $[Co(CN)_5(OONO)]^{3-}$.[61] Additionally Richter-Addo et al.[60] found that the rate of the reaction of the picket fence porphyrin complex [Fe(tpivpp)(NO)] with air in $CHCl_3$ solution is enhanced by light. A control experiment in the absence of regular laboratory light showed that light has no effect on the observed product ratio for our system, Supporting Information, Figure S17.

It occurred to us that as for other cob(III)alamins with inorganic ligands bound at the β-axial site, Co(III)-$ONOO^-$ is in equilibrium with H_2OCbl^+/HOCbl plus ONOO(H) at pH 7.4, and that decomposition of the intermediate may therefore occur via hydrolysis of Co-$ONOO^-$. However, a comparison of the observed rate constants for the reaction between NOCbl and O_2 at pH 10.40 (k_{obs} = 0.05−0.35 s^{-1}, Supporting Information, Figure S2) and the observed rate constant for ONOO(H) decomposition at pH 10.40 ($k_{obs} = 4.68 \times 10^{-4}$ s^{-1}; Supporting Information, Figure S18) makes it clear that decomposition via this pathway is not occurring. Given that $ONOO^-$ is so stable in aqueous solution,[62] it is likely that the metal center substitutes for the proton of ONOOH, to assist in the decomposition of Co(III)-bound peroxynitrite.[50,63] However, note that the proton of ONOOH is located on an O atom, whereas it is likely that *N*-bound Co(III)-N(O)OO^- is initially formed. Whether or not this latter complex isomerizes to *O*-bound Co(III)-$OONO^-$ prior to undergoing O−O bond homolysis of the ligand to give $^{\bullet}NO_2$ and $^{\bullet}OH$ is not known.

Phenol and tyrosine are established trapping agents for $^{\bullet}NO_2$ and $^{\bullet}OH$. Aerial oxidation of NOCbl in the presence of phenol (0.10 M) gave nitrated phenol products (<1%), providing evidence for a $^{\bullet}NO_2$ intermediate. In the presence of a Tyr trap OH-Tyr was detected, consistent with formation of a $^{\bullet}OH$ intermediate. HPLC and mass spectrometry also provided

Scheme 4. Proposed Reaction Pathways for the Reaction between NOCbl and O_2

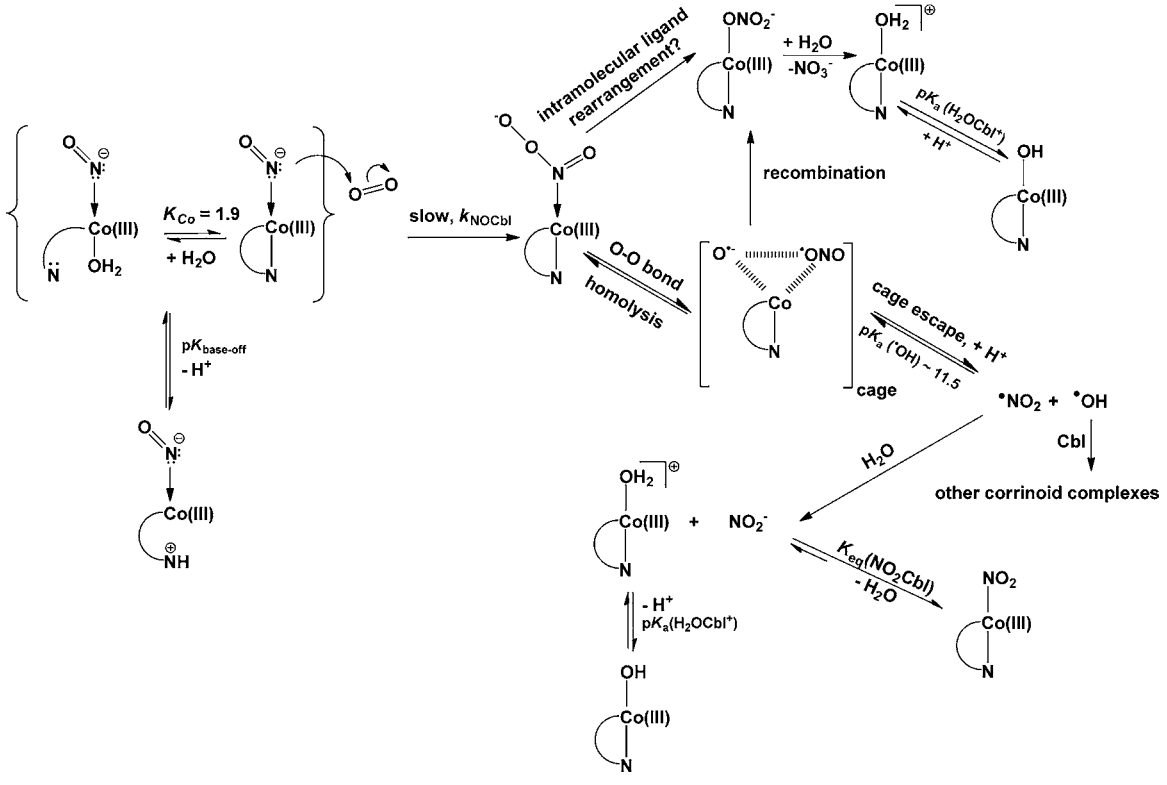

dx.doi.org/10.1021/ic401975f | *Inorg. Chem.* 2013, 52, 11608−11617

evidence for formation of a small amount of a corrinoid species with two less H atoms than Cbl, consistent with attack by $^{\bullet}OH$ on the corrin ring.

Scheme 4 summarizes the proposed reaction pathways for the reaction between NOCbl and O_2. In this scheme the rate-determining reaction of NOCbl with O_2 to form an *N*-bound peroxynitritocobalamin intermediate is followed by O−O bond homolysis of the Co(III)-bound peroxynitrite ligand and ligand isomerization. It is not clear to us whether ligand isomerization occurs via direct intramolecular ligand rearrangement in addition to O−O bond homolysis followed by radical recombination. In any event, ligand isomerization leads to formation of nitratocobalamin (NO_3Cbl), which rapidly hydrolyzes to H_2OCbl^+.[28] O−O bond homolysis results in the formation of caged $^{\bullet}NO_2$ and $^{\bullet}OH$. Theoretical studies show that $ONOO^-$ decomposes to $^{\bullet}NO_2$ and $^{\bullet}O^-$;[64] the latter is rapidly protonated to form $^{\bullet}OH$ ($pK_a(^{\bullet}OH) \sim 11.5$[65]). Upon release from the cage $^{\bullet}NO_2$ reacts rapidly with itself and H_2O to produce NO_2^-,[55,66] which then substitutes the β-axial H_2O ligand of H_2OCbl^+ to form NO_2Cbl. The yields of the phenol and Tyr - trapped $^{\bullet}NO_2$ and $^{\bullet}OH$ products (<1%) are considerably less than those observed for spontaneous ONOOH decomposition under the neutral pH conditions of this study, suggesting that Cbl can also trap these species. In support of this, a novel corrinoid complex is observed in the HPLC chromatogram with a mass which is 2 units smaller than Cbl itself, consistent with scavenging of $^{\bullet}OH$ by the corrin ring. $^{\bullet}OH$ could potentially also react with the corrin ring of the Cbl within the caged complex.

CONCLUSIONS

Kinetic and mechanistic studies on the reaction between NOCbl and O_2 show that the reaction is rapid, and proceeds via an associative mechanism with the formation of a peroxynitritocob(III)alamin intermediate, $Co(III)\text{-}N(O)OO^-$. The intermediate undergoes O−O bond homolysis and ligand isomerization to ultimately yield NO_2Cbl and H_2OCbl^+/HOCbl, respectively. Ligand isomerization may potentially occur independent of O−O bond homolysis. Formation of small amounts of $^{\bullet}OH$ and $^{\bullet}NO_2$ intermediates is demonstrated using phenol and tyrosine radical traps and ESI-MS characterization of a corrinoid complex with 2 H less than the Cbl unit. This study gives a detailed mechanistic analysis of the seemingly simple reaction between the biologically important cobalamin NOCbl and oxygen. The oxygen concentration in cells varies from 4 to 40 μM.[67] Assuming a concentration of 20 μM, the half-life for the reaction of NOCbl with O_2 is ∼1 min (25 °C). In air the half-life for NOCbl decomposition is ∼5 s.

ASSOCIATED CONTENT

Supporting Information

Additional kinetic data, ^{1}H NMR spectra, and HPLC and ESI-MS chromatograms; Figures S1−S18. This material is available free of charge via the Internet at http://pubs.acs.org.

AUTHOR INFORMATION

Corresponding Author

*E-mail: nbrasch@kent.edu.

Notes

The authors declare no competing financial interest.

ACKNOWLEDGMENTS

The authors gratefully acknowledge the assistance of Dr. Donald L. Dick (Department of Chemistry, Colorado State University, CO, U.S.A.) with mass spectrometry experiments. This material is based upon work supported by the U.S. National Science Foundation under Grant CHE-0848397.

REFERENCES

(1) Dennis, J. S. *Biochim. Biophys. Acta* **1999**, *1411*, 217.
(2) Ignarro, L. J.; Cirino, G.; Casini, A.; Napoli, C. *J. Cardiovasc. Pharmacol.* **1999**, *34*, 879.
(3) Bian, K.; Murad, F. *Front. Biosci.* **2003**, *8*, d264.
(4) Hassanin, H. A.; Hannibal, L.; Jacobsen, D. W.; Brown, K. L.; Marques, H. M.; Brasch, N. E. *Dalton Trans.* **2009**, 424.
(5) Nicolaou, A.; Kenyon, S. H.; Gibbons, J. M.; Ast, T.; Gibbons, W. A. *Eur. J. Clin. Invest.* **1996**, *26*, 167.
(6) Kambo, A.; Sharma, V. S.; Casteel, D. E.; Woods, V. L.; Pilz, R. B.; Boss, G. R. *J. Biol. Chem.* **2005**, *280*, 10073.
(7) Brouwer, M.; Chamulitrat, W.; Ferruzzi, G.; Sauls, D.; Weinberg, J. *Blood* **1996**, *88*, 1857.
(8) Carmen, W. *Med. Hypotheses* **2006**, *67*, 124.
(9) Padovani, D.; Banerjee, R. *Biochemistry* **2006**, *45*, 9300.
(10) Wolak, M.; Zahl, A.; Schneppensieper, T.; Stochel, G.; van Eldik, R. *J. Am. Chem. Soc.* **2001**, *123*, 9780.
(11) Zheng, D.; Birke, R. L. *J. Am. Chem. Soc.* **2001**, *123*, 4637.
(12) Wheatley, C. *J. Nutr. Environ. Med.* **2007**, *16*, 181.
(13) Jiang, F.; Li, C. G.; Rand, M. J. *Eur. J. Pharmacol.* **1997**, *340*, 181.
(14) Rand, M. J.; Li, C. G. *Eur. J. Pharmacol.* **1993**, *241*, 249.
(15) Greenberg, S. S.; Xie, J.; Zatarain, J. M.; Kapusta, D. R.; Miller, M. J. *J. Pharmacol. Exp. Ther.* **1995**, *273*, 257.
(16) Bauer, J. A.; Lupica, J. A.; Schmidt, H.; Morrison, B. H.; Haney, R. M.; Masci, R. K.; Lee, R. M.; DiDonato, J. A.; Lindner, D. J. *PLoS ONE* **2007**, *2*, e1313.
(17) Wolak, M.; Stochel, G.; van Eldik, R. *Inorg. Chem.* **2005**, *45*, 1367.
(18) Hannibal, L.; Smith, C. A.; Jacobsen, D. W.; Brasch, N. E. *Angew. Chem., Int. Ed.* **2007**, *46*, 5140.
(19) Weil, M.; Abeles, R.; Nachmany, A.; Gold, V.; Michael, E. *Cell Death Differ.* **2004**, *11*, 361.
(20) Nicolaou, A.; Waterfiesd, C. J.; Kenyon, S. H.; Gibbons, W. A. *Eur. J. Biochem.* **1997**, *244*, 876.
(21) Danishpajooh, I. O.; Gudi, T.; Chen, Y.; Kharitonov, V. G.; Sharma, V. S.; Boss, G. R. *J. Biol. Chem.* **2001**, *276*, 27296.
(22) Suarez-Moreira, E.; Hannibal, L.; Smith, C. A.; Chavez, R. A.; Jacobsen, D. W.; Brasch, N. E. *Dalton Trans.* **2006**, 5269.
(23) Trogler, W. C.; Marzilli, L. G. *Inorg. Chem.* **1974**, *13*, 1008.
(24) Vlasova, E. A.; Hessenauer-Ilicheva, N.; Salnikov, D. S.; Kudrik, E. V.; Makarov, S. V.; van Eldik, R. *Dalton Trans.* **2009**, 10541.
(25) Barker, H. A.; Smyth, R. D.; Weissbach, H.; Toohey, J. I.; Ladd, J. N.; Volcani, B. E. *J. Biol. Chem.* **1960**, *235*, 480.
(26) Pinto, E.; Petissca, C.; Amaro, L. F.; Pinho, O.; Ferreira, I. M. P. L. V. O. *J. Liq. Chromatogr. Relat. Technol.* **2010**, *33*, 591.
(27) Ferreira, I. M. P. L. V. O.; Silva, S. *Talanta* **2008**, *74*, 1598.
(28) Pratt, J. M. *Inorganic Chemistry of Vitamin B_{12}*; Academic Press: New York, 1972; p 280.
(29) Brasch, N. E.; Finke, R. G. *J. Inorg. Biochem.* **1999**, *73*, 215.
(30) Clarkson, S. G.; Basolo, F. *Inorg. Chem.* **1973**, *12*, 1528.
(31) Ford, P. C.; Lorkovic, I. M. *Chem. Rev.* **2002**, *102*, 993.
(32) Herold, S.; Koppenol, W. H. *Coord. Chem. Rev.* **2005**, *249*, 499.
(33) Frech, C. M.; Blacque, O.; Schmalle, H. W.; Berke, H. *Dalton Trans.* **2006**, 4590.
(34) Arnold, E. V.; Bohle, D. S. *Methods Enzymol.* **1996**, *269*, 41.
(35) Park, G. Y.; Deepalatha, S.; Puiu, S. C.; Lee, D.-H.; Mondal, B.; Narducci, S. A. A.; del Rio, D.; Pau, M. Y. M.; Solomon, E. I.; Karlin, K. D. *J. Biol. Inorg. Chem.* **2009**, *14*, 1301.
(36) Herold, S.; Exner, M.; Nauser, T. *Biochemistry* **2001**, *40*, 3385.
(37) Nemes, A.; Pestovsky, O.; Bakac, A. *J. Am. Chem. Soc.* **2001**, *124*, 421.

(38) Wick, P. K.; Kissner, R.; Koppenol, W. H. *Helv. Chim. Acta* **2000**, *83*, 748.
(39) Ramezanian, M. S.; Padmaja, S.; Koppenol, W. H. *Chem. Res. Toxicol.* **1996**, *9*, 232.
(40) Mukherjee, R.; Brasch, N. E. *Chem.—Eur. J.* **2011**, *17*, 11805.
(41) Beckman, J. S. *Chem. Res. Toxicol.* **1996**, *9*, 836.
(42) Pietraforte, D.; Salzano, A. M.; Marino, G.; Minetti, M. *Amino Acids* **2003**, *25*, 341.
(43) Santos, C. X. C.; Bonini, M. G.; Augusto, O. *Arch. Biochem. Biophys.* **2000**, *377*, 146.
(44) Lymar, S. V.; Jiang, Q.; Hurst, J. K. *Biochemistry* **1996**, *35*, 7855.
(45) Bartesaghi, S.; Valez, V.; Trujillo, M.; Peluffo, G.; Romero, N.; Zhang, H.; Kalyanaraman, B.; Radi, R. *Biochemistry* **2006**, *45*, 6813.
(46) Bonnett, R.; Cannon, J. R.; Clark, V. M.; Johnson, A. W.; Parker, L. F. J.; Smith, E. L.; Todd, A. *J. Chem. Soc.* **1957**, 1158.
(47) Bonnett, R. *Chem. Rev.* **1963**, *63*, 573.
(48) Reference *28*, p 193.
(49) Matthews, J. H. *Blood* **1997**, *89*, 4600.
(50) Goldstein, S.; Lind, J.; Merényi, G. *Chem. Rev.* **2005**, *105*, 2457.
(51) Kurtikyan, T. S.; Eksuzyan, S. R.; Hayrapetyan, V. A.; Martirosyan, G. G.; Hovhannisyan, G. S.; Goodwin, J. A. *J. Am. Chem. Soc.* **2012**, *134*, 13861.
(52) Maiti, D.; Lee, D.-H.; Narducci, S. A. A.; Pau, M. Y. M.; Solomon, E. I.; Gaoutchenova, K.; Sundermeyer, J.; Karlin, K. D. *J. Am. Chem. Soc.* **2008**, *130*, 6700.
(53) Kalita, A.; Kumar, P.; Mondal, B. *Chem. Commun.* **2012**, *48*, 4636.
(54) Szabo, C.; Ischiropoulos, H.; Radi, R. *Nat. Rev. Drug Discovery* **2007**, *6*, 662.
(55) Goldstein, S.; Merényi, G. In *Methods in Enzymology*; Robert, K. P., Ed.; Academic Press: New York, 2008; Vol. *436*, p 49.
(56) Koppenol, W. H.; Bounds, P. L.; Nauser, T.; Kissner, R.; Rueegger, H. *Dalton Trans.* **2012**, *41*, 13779.
(57) Koppenol, W. H.; Moreno, J. J.; Pryor, W. A.; Ischiropoulos, H.; Beckman, J. S. *Chem. Res. Toxicol.* **1992**, *5*, 834.
(58) Lippard, S. J.; Berg, J. M. *Principles Bioinorganic Chemistry*; University Science Books: Mill Valley, CA, 1994.
(59) Ishii, K.; Aoki, K. *Anal. Chem.* **1983**, *55*, 604.
(60) Cheng, L.; Powell, D. R.; Khan, M. A.; Richter-Addo, G. B. *Chem. Commun.* **2000**, 2301.
(61) Wick, P. K.; Kissner, R.; Koppenol, W. H. *Helv. Chim. Acta* **2001**, *84*, 3057.
(62) Al-Ajlouni, A. M.; Gould, E. S. *Inorg. Chem.* **1996**, *35*, 7892.
(63) Herold, S. *FEBS Lett.* **1999**, *443*, 81.
(64) Merényi, G.; Lind, J.; Goldstein, S.; Czapski, G. *J. Phys. Chem. A* **1999**, *103*, 5685.
(65) Poskrebyshev, G. A.; Neta, P.; Huie, R. E. *J. Phys. Chem. A* **2002**, *106*, 11488.
(66) Merényi, G.; Lind, J. *Chem. Res. Toxicol.* **1998**, *11*, 243.
(67) Fandrey, J.; Gorr, T. A.; Gassmann, M. *Cardiovasc. Res.* **2006**, *71*, 642.